Preparation and Electrothermal Properties of Graphene Electrothermal Composite Floor

Jiawei Zhang, Tian Su, Xin Leng, Bo Peng, Jiacheng Tang, Zhe Han, Shuyang Lin, Peilong Yu, Song Zhang, and Chunmei Yang *

Conventional electrothermal floors suffer from low heating efficiency, uneven temperature distribution across the floor surface, local overheating, and severe heat accumulation. In order to improve the heating performance, an electrothermal composite floor with graphene as the heating layer was fabricated. The relationship between time and temperature rise, the relationship between power density and temperature rise, running stability, and surface temperature distribution were investigated and analyzed after heating, and the surface temperature profiles were simulated in two and three dimensions. The results were compared with the carbon fiber electrothermal composite floor and the resistance wire electrothermal composite floor. The results indicated that the temperature of the graphene electrothermal composite floor rose to 27.1 °C, the electrothermal conversion efficiency reached 90.1% after 40 min of electrification, and the temperature distribution unevenness was 4.4 °C, which were better than the carbon fiber electrothermal composite floor and the resistance wire electrothermal composite floor. The graphene electrothermal composite floor exhibited high heating performance, thus aiding the development and manufacture of such composite flooring.

DOI: 10.15376/biores.18.4.6929-6943

Keywords: Graphene; Electrothermal composite floor; Electrothermal performance; Surface temperature

*Contact information: College of Computer and Control Engineering, Northeast Forestry University, Harbin 150040 China; *Corresponding author: 962620684@qq.com*

INTRODUCTION

The increased demand for heating comfort has led to the emergence of a new heating method, electric floor heating. The electrothermal wooden floor with integrated electric heating layer is made up of a wooden substrate and an encapsulated electric heating material. It can be heated after being energized. The structure of this type of floor is similar to a sandwich, composed of multiple layers of functional materials and an electric heating element. When compared to electrothermal cement and electrothermal ceramic tile, electric floor heating has many advantages, including fast heating speed, high comfort, energy efficiency, safety, and eco-friendliness.

However, the traditional electrothermal floors present issues such as low heating efficiency, uneven temperature distribution on the floor surface, local overheating, and severe heat accumulation (Zhou *et al.* 2018). As a result, researchers are investigating the use of novel materials and processes to manufacture electrically heated floors. Liang *et al.* (2022) studied the composite manufacturing process of electrothermal floor with a built-in carbon fiber heating layer. Ti *et al.* (2022) prepared a carbon fiber electrothermal floor and explored its electrothermal performance, which promoted the development of the

electrothermal floor industry. Liu has proposed that when preparing an electrothermal floor, wood species with high density, high thermal conductivity, and high strength should be used as the substrate (Liu *et al.* 2023). The electric heating floor generally consists of a facing layer, an upper substrate, a heating layer, a lower substrate, and a thermal insulation layer (Liang *et al.* 2018). The heating layer of the electric heating floor usually uses resistance wire, conductive ink, carbon crystal electric heating sheet, carbon fiber cable, carbon fiber heating paper (Bao *et al.* 2020), graphene heating film, and so on as heating materials.

A graphene electrothermal floor using graphene heating film as the heating layer provides more evenly distributed heating and a higher efficiency of low-temperature thermal radiation (Chen *et al.* 2022). Graphene is a two-dimensional nanomaterial made of a single layer of carbon atoms arranged in a hexagonal honeycomb lattice. Single layer graphene has a thermal conductivity that can reach up to 5300 W/(m·K). Recently, graphene has also been utilized for heating materials. Graphene can emit far-infrared light with a wavelength ranging from 6 to 15 μm. This light has been shown to have positive medical and physiotherapeutic effects on the human body (Wang 2021). Graphene has good thermal comfort and economic benefits for indoor heating. Once the graphene heating layer in an electrothermal floor is energized, the heat is evenly transferred to the indoor air through infrared radiation, creating an indoor environment that meets human comfort with its cool head and warm feet (Feng 2017). Yang *et al.* (2023) designed a composite graphene heating floor and described the heat transfer process of the electric heating floor.

Long-term use or accidental over-coverage of electric heating floors can still cause problems such as local overheating, severe heat accumulation, and uneven temperatures. The heating performance of electric floors can be enhanced by using various thermally-conductive materials for their production. The installation of a flat aluminum core radiator plate on the electrothermal floor has been shown to improve the temperature uniformity over the floor surface (Zhou *et al.* 2019). The uniformity of the surface temperature is improved by the use of graphite films as a thermal conductive material. It also can result in a more uniform heat effect and reduced the level of heat accumulation on the surface after heating the electrothermal parquet flooring substrate (Liang *et al.* 2019).

The study designed a five-layer electrothermal composite floor composed of eucalyptus plywood as substrate, graphene electrothermal film as the heating element, graphite paper as the thermal conductive material, and low formaldehyde modified urea-formaldehyde resin adhesive as the bonding agent. The relationship between time and temperature rise, the relationship between power density and temperature rise, running stability, and surface temperature distribution were investigated and analyzed after heating, and the surface temperature profiles were simulated in two and three dimensions. A comparison between carbon fiber and resistance wire electrothermal composite floors revealed that the graphene electrothermal composite floor demonstrated a higher electro-thermal conversion efficiency and temperature uniformity. In addition, a new type of graphene electrothermal composite floor was constructed in this study with the aim of improving surface temperature uniformity, heat transfer efficiency and reducing safety hazards, while providing technical support for the development and production of electrothermal composite flooring.

EXPERIMENTAL

Materials and Equipment

Eucalyptus solid wood panels were provided by Jiangsu Fuqiang Board Industry Co. (Wuxi, China). Graphite thermal conductive paper was purchased from Beijing Jinglongte Carbon Graphite Co. (Beijing, China). Low formaldehyde modified urea formaldehyde resin adhesive was purchased from Qingjun Building Materials Co. (Suzhou, China).

As shown in Fig. 1, various heating materials have been used to prepare electrothermal composite floors. The graphene heating film was made of graphene, a conductive silver paste, a PTC functional material, and a high temperature resistant polyvinyl chloride transparent film. The two sides of the graphene heater film were connected by wires extending outwards. The graphene film was purchased from Qingdao Dongdi Warm Installation Engineering Co. (Qingdao, China). The carbon fiber heating film was made of carbon fiber, high temperature resistant polyvinyl chloride transparent film, and pure copper electrode, and was purchased from Zhuge Liang Intelligent Electronics Co. (Shenzhen, China). The resistance wire heating sheet was composed of resistance wire and aluminum foil, and was purchased from Xiamen Vitek Electronics Co. (Xiamen, China).

Fig. 1. Materials of heating layer

Structure Design and Process Flow of Electrothermal Composite Floor

Ti *et al*. (2022) prepared a composite floor, compared to other floors, which exhibited good heating performance. The side structure of the prepared electrothermal composite floor is shown in Fig. 2. There were five layers of graphene electrothermal composite floor, including a panel layer, thermal conductivity layer, upper substrate layer, heating layer, and a lower substrate layer from top to bottom.

The amount of glue applied to the plywood was 80 g/m^2, and it was painted manually with a brush. The panel and the top and bottom substrates were painted separately on one side, with the principle that there should be no glue spillage at the edge of the panel after hot pressing. The board was assembled in the order shown in Table 1. After aging for 20 min, the block was set in place. The composite was hot-pressed to produce the electrothermal composite floor with a double-sided press. The amount of sizing on one side was constant, the hot-pressing pressure was set to 1.2 MPa, and the pressing temperature was not set. First, the electrothermal floor substrate was cold pressed for 30 min according to the above structure, and then the hot-pressing pressure was set to 1.2 MPa for 6 min at 130 °C. The prepared electrothermal floor was placed in an oven with constant temperature and humidity for 24 h to ensure the stability of the floor structure. At the same time, an electrothermal composite floor with a built-in resistance wire heating sheet and a carbon fiber heating film as the heating layer was prepared as a control.

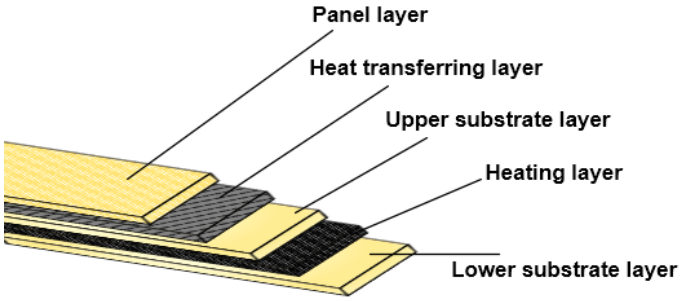

Fig. 2. Electrothermal composite floor structure schematic diagram

Table 1. Materials and Dimensions of Each Layer of the Electrothermal Composite Floor

Names of Each Layer	Materials	Breadth	Thickness
Panel layer	Eucalyptus veneer	500 mm × 250 mm	3 mm
Heat transferring layer	Graphite paper	500 mm × 250 mm	0.3 mm
Upper substrate layer	Eucalyptus veneer	500 mm × 250 mm	3 mm
Heating layer	Graphene heating film/ Carbon fiber heating film/ Resistance wire heating sheet	500 mm × 250 mm	1mm/ 1mm/ 1mm
Lower substrate layer	Eucalyptus plywood	500 mm × 250 mm	5 mm

Electrothermal Performance Test of Electrothermal Composite Floor

Six high-density thermal insulation extruded panels (polystyrene foam panels) of 50 cm x 50 cm x 3 cm were selected. The sides of the extruded panels are covered with high-temperature aluminium foil. An adiabatic indoor environment was constructed and the electrothermal performance of the composite floor was studied. The test chamber was used to reduce the influence of external environmental factors on the temperature data collected.

As shown in Fig. 3, the electrothermal composite floor was placed in the center of the test chamber. The purpose of the test was to investigate the heating situation of the composite floor in the small room and to test its electrothermal performance and heating laws.

Relationship between temperature and time

According to the GB/ T7287 standard (2008), nine temperature measurement points, as shown in Fig. 4, were set on the surface of the floor. The four sides of the inner frame in the figure were the long and wide sides of the floor, 10 mm inward. The inner frame was divided into 9 rectangles with the same area, and the center point of each area was taken as the temperature measurement point. The graphene electrothermal composite floor was subjected to a normal voltage of 220 V, and the temperature recorder (MIK-R200T, Hangzhou Miko Sensing Technology Co., Hangzhou, China) was used to collect the temperature data of the floor surface 40 min after energization. K-type thermocouples were attached to the temperature measurement points and the temperature data was

recorded every 10 seconds using a temperature recorder to analyze the temperature rise law. The average value of 9 temperature measurement points was taken as the average temperature of each plate, and the temperature-time effect curve was plotted.

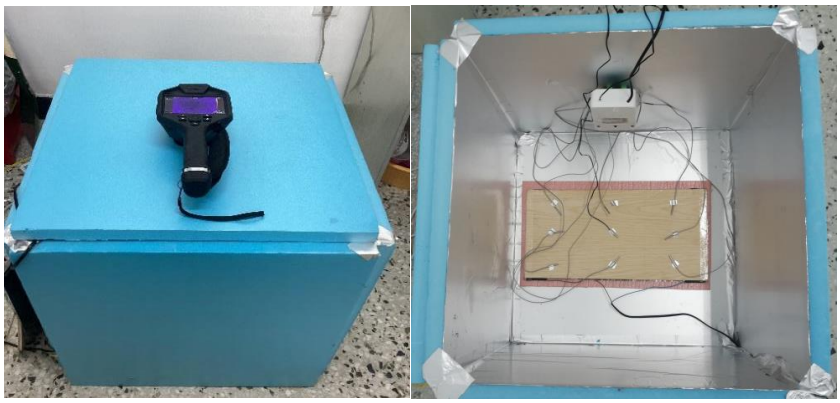

Fig. 3. Electrothermal composite floor heating performance tester diagram

Relationship between power density and temperature

The input voltage of the electrothermal composite floor was adjusted by the single-phase AC voltage regulator (TDGC2-1, regulating range of 0-300V, Zhejiang Zhengtai Electric Co., Leqing, China), to input different power densities. Five power densities of 100, 150, 200, 250, and 300 W/m^2 were set. The temperature data of the surface of the composite floor were collected by the temperature detector, and the temperature rise within 100 min was recorded. The recording time interval was 10 seconds.

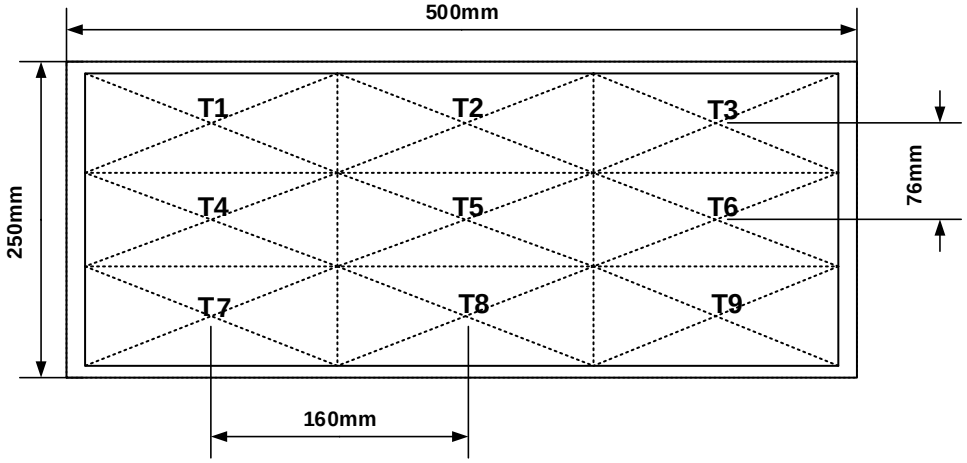

Fig. 4. The distribution map of temperature measurement points on the surface of electrothermal composite floor

Temperature distribution of the panel surface

An infrared thermal imager was used to check the temperature distribution of the floor surface 40 min after electrification. The infrared thermal imager (FOTRIC322, Shanghai Thermovision Co., Shanghai, China), was recorded at an interval of 60 seconds, and the temperature data were extracted from it. The analysis of the temperature distribution law was performed with the software AnalyzIR.

Running stability

To investigate the running stability of the floor, the start-stop reciprocating operation of the electrothermal composite floor was tested within 10 h when the electrothermal floor was working normally. During the test, the start and stop of the electric heating floor was controlled by the center point temperature of the electric heating composite floor. When the center point temperature reached 50 °C, the power was cut off, and when the center point temperature was reduced to 25 °C, the device was turned on. This was repeated until the experiment had lasted 10 h, when it was stopped. The temperature detector was used to collect the floor surface temperature data at the point T5 shown in Fig. 4 with a data collection time interval of 1 minute.

Electro-thermal radiation conversion efficiency

The rated working voltage of 220 V was applied to the electrothermal composite floor. When the power was switched on and the temperature rose to equilibrium, the value of electrical power at that time was recorded. The distance between the infrared thermal imager probe and the electric heating composite floor was appropriately adjusted so that the electric heating floor surface essentially filled the thermal imager field of view. The bolometer emissivity correction value was set to 1.0000. The average radiation temperature T_r at the radiant surface of the heater was measured by an infrared thermal imager, and the electric heating conversion efficiency formula was as shown in Eq.1,

$$\eta = \frac{S\sigma\left(T_r^4 - T_0^4\right)}{P_e} \times 100\% \quad (1)$$

where η is electric-thermal radiation conversion efficiency (%), P_e is the measured electric power (W), T_r is the average ejecting temperature on the absolute scale (K), T_0 is ambient temperature (K), and σ is the Steffan-Boltzmann constant .

Within the voltage range of 0 to 220V, the heating temperature was measured at each interval of 5 V, respectively, and the relationship between voltage and thermal efficiency was obtained in the MATLAB software according to the calculation formula of infrared radiation thermal efficiency in the national GB/T 7287 standard (2008).

RESULTS AND DISCUSSION

Relationship between Time and Temperature Rise of Graphene Electrothermal Composite Floor

With the increase of the energization time, the temperature change of the graphene electrothermal composite floor was obtained, and the results are shown in Fig. 5. After the onset of electrification, the surface and bottom temperatures of the graphene electrothermal composite floor showed an increasing trend with time. The temperature increase of the panel surface and the temperature increase of the panel bottom were exponentially related to time. An exponential curve relationship was found between temperature rise and the time of electrification *via* data fitting (Eq. 2 for the surface and Eq. 3 for the bottom). After about 40 min of electrification, the temperature of the surface and the bottom of the graphene electrothermal composite floor tended to stabilize. The temperature rise of the surface reached 25.5 °C, and the temperature of the bottom reached 27.3 °C, which was higher than the requirements of the GB/T 41547 standard (2022). This indicated that the

graphene electrothermal composite floor exhibited good heating performance.

$$T = 25.97 - 26.55e^{-\frac{t}{12.29}}, (R^2 = 0.984) \quad (2)$$

$$T = 27.58 - 27.78e^{-\frac{t}{10.41}}, (R^2 = 0.998) \quad (3)$$

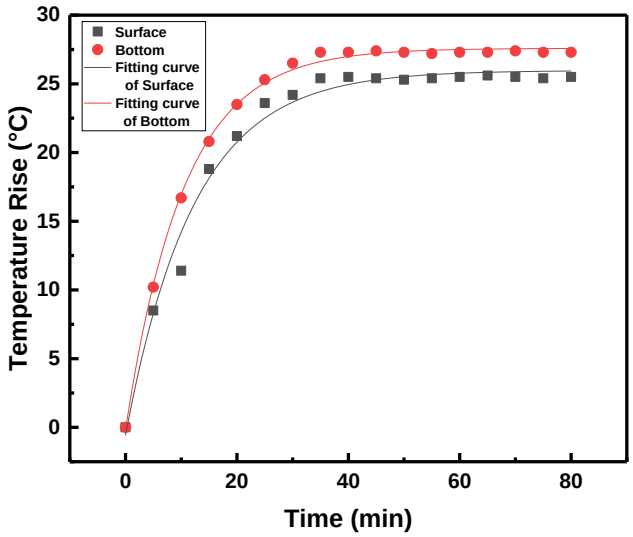

Fig. 5. Temperature rise-time diagram of graphene electrothermal composite floor and bottom

As can be seen from Fig. 5, the temperature of the graphene electrothermal composite floor increased more rapidly during the first 20 min of electrification. This was because the overall temperature of the electrothermal floor was lower in the initial phase. The heat generated by the graphene heating film causes the surface temperature of the electrothermal floor to rise rapidly, while the surrounding ground and ambient temperatures remained at the initial temperature values. The electrothermal floor transferred its own heat to the environment to increase the ambient temperature, which will then gradually increase. When the time reached 40 min, the heat exchange and heat convection between the graphene electrothermal composite floor and the surrounding environment reached a dynamic equilibrium, and the overall temperature of the graphene electrothermal composite floor tended to equilibrate and eventually remained stable. The temperature of the bottom of the plate was higher than that of the surface of the plate because the surface of the electrothermal composite floor was directly exposed to the air and always transferred heat with the air, while the bottom of the plate was directly in contact with the heat insulation film, and the temperature of the bottom of the plate was slightly increased due to the heat storage effect.

Relationship between Power Density and Temperature Rise of Graphene Electrothermal Composite Floor

As shown in Fig. 6a, time-effect plots of the temperature rise of the graphene electrothermal composite floor under five different power densities of 100, 150, 200, 250, and 300 W/m^2. The temperature of the graphene electrothermal composite floor with input power densities of 200, 250, and 300 W/m^2 rose rapidly after energization, and the temperature of the floor surface stabilized after 40 min. The temperature increase was 27.9, 34, and 40.2 °C, respectively. The temperature of the graphene electrothermal composite floor with input power densities of 100 and 150 W/m^2 increased slowly after energization.

After 60 min, the temperature of the floor surface was stable, and the temperature increase was 13.6 and 21.2 °C, respectively. The surface temperature increase of the electrothermal composite floor reached 27.3 °C at a voltage of 220 V (195 W/m^2). Figure 6b shows a linear relationship between the surface temperature rise and the power density of the electrothermal composite floor. The surface temperature increased uniformly with the input power density, and the fitting function is shown in Eq. 4.

$$y = 0.98 + 0.132x \ , (R^2 = 0.9979) \quad (4)$$

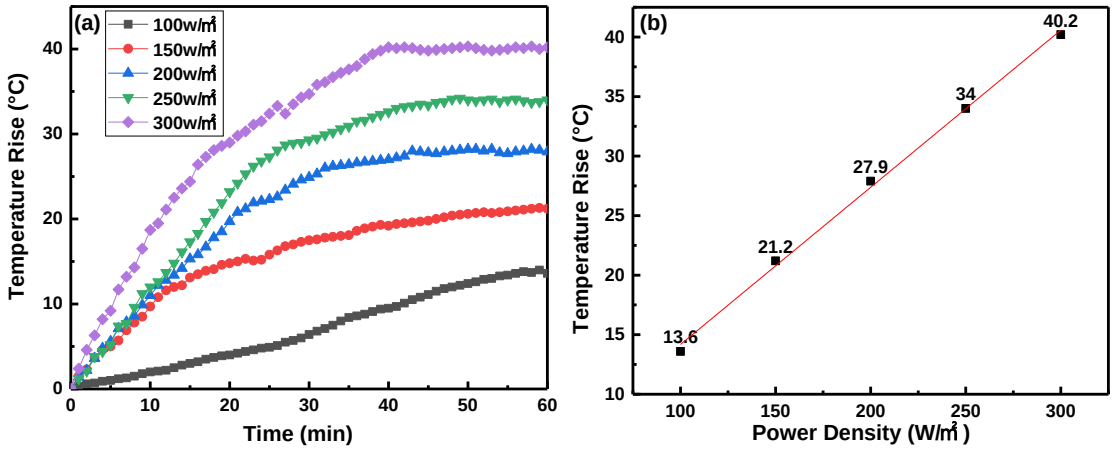

Fig. 6. (a) Relationship between the time and temperature rise of the electric heating floor under various power densities; (b) relationship between the temperature rise and power density

Table 2. Temperature Variation Range of Graphene Electrothermal Composite Floor with Different Power Density

Temperature Rising Time (Min)	Temperature Change Range (°C)				
	Power density 100 W/m^2	Power density 150 W/m^2	Power density 200 W/m^2	Power density 250 W/m^2	Power density 300 W/m^2
10	2	9.7	11	12	18.7
20	4	14.8	19.7	23.2	29
30	6.4	17.5	24.9	29.3	34.7
40	9.5	19.2	27	32.6	40.2
50	12.4	20.6	28.2	34	40.3
60	13.6	21.2	27.9	34	40.2

As shown in Table 2, as the input power density increased, the temperature variation of the plate surface increased and the heating time decreased. According to the law of conservation of energy (Li 2018), the heat generated by the graphene heating film is equal to the sum of the heat stored in the graphene electric heating floor itself and the heat transferred to the environment (Song *et al.* 2017; Zhou *et al.* 2018). The heat generated by the graphene heating film could be calculated as follows (Eq. 5),

$$Q = Q_c + Q_s \quad (5)$$

where Q is the heat generated by the graphene heating film, Q_c is the heat stored in the wood-based graphene electrothermal composite floor itself, and Q_s is the heat transferred to the environment. The values of Q, Q_c and Q_s could be determined as follows,

$$Q = Pt \quad (6)$$

$$Q_c = cm\Delta T \quad (7)$$

$$Q_s = Sa_t\Delta T \quad (8)$$

where P, t, c, m, S, and a_t are the power, time, specific heat capacity, mass, effective heating area, and heat transfer coefficient of the electrothermal solid wood composite floor.

$$\Delta T = \frac{Pt}{cm+Sa_t} \quad (9)$$

In Eq. 9, the temperature variation of the graphene electrothermal composite floor was positively correlated with the input power density and the energization time, and with the specific heat capacity, mass and effective heating area of the electrothermal solid wood composite floor. As the input power density increased, the temperature increase of the electrothermal composite floor changed accordingly. By adjusting the power density of the input electrothermal composite floor, the temperature control of the graphene electrothermal composite floor can be easily and quickly achieved.

Running Stability of Graphene Electrothermal Composite Floor

As can be seen in Fig. 7a, the average temperature variation of the graphene electrothermal composite floor was plotted for 10 h of continuous operation.

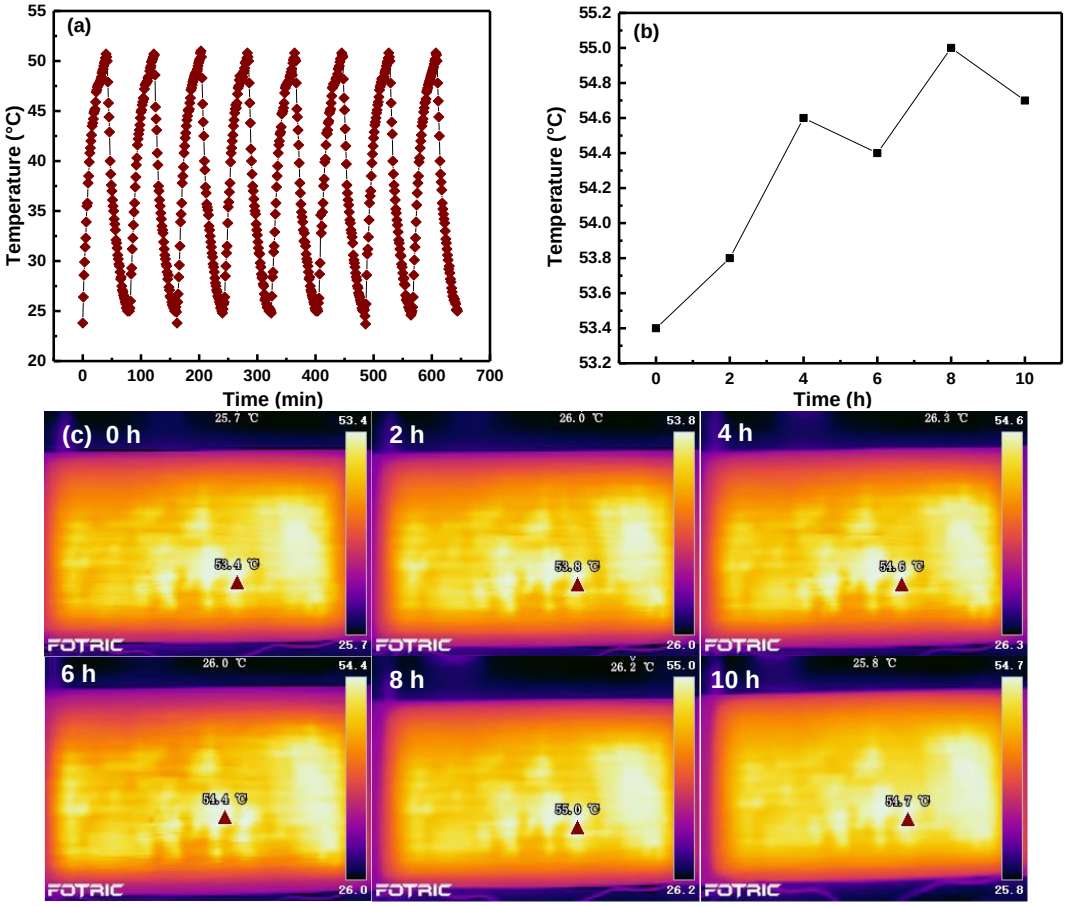

Fig. 7. (a) The reciprocating operation condition of graphene electrothermal composite floor in 10 h; (b) The surface peak temperature variation curve of graphene electrothermal composite floor in 10 h; (c) The surface infrared thermal image of graphene electrothermal composite floor in 10 h

The highest average temperature during the operation did not exceed 51 °C, and the lowest was not less than 23.7 °C. There were no unusual temperatures. As shown in Fig. 7b, the surface peak temperature of the graphene electrothermal composite floor was below 55 °C after continuous energization for 10 h. As can be seen from the surface infrared thermal image in Fig. 7c, the surface temperature distribution of the floor was uniform, and there were no local high temperature phenomenon. The floor had a stable running performance.

The Relationship between Time and Temperature of Three Kinds of Electrothermal Composite Floor

Figure 8 shows the temperature-time effect curves of graphene electrothermal composite floor, resistance wire electrothermal composite floor, and carbon fiber electrothermal composite floor after power on and power off. After power on, the average temperature of the three electrothermal floors was recorded separately. When the surface temperature of the electrothermal floor tended to stabilize, the power supply was cut off to stop the power flow, and a decrease in the average temperature of the three electrothermal floors was recorded. The heating rate of the resistance wire electrothermal composite floor was relatively fast, taking 30 min, while that of the graphene electrothermal composite floor was moderate, taking 42 min. The heating rate of carbon fiber electrothermal composite floor was the slowest, which takes 54 min. After the power was turned off, the carbon fiber electrothermal composite floor took 20 min to return to the initial temperature, the resistance wire electrothermal composite floor took 35 min to return to the initial temperature, and the graphene electrothermal composite floor took 38 min to return to the initial temperature. This indicated that the carbon fiber electrothermal composite floor had a poor heat storage capacity and poor heat retention, while the graphene electrothermal composite floor had the longest heat dissipation time, ample heat storage capacity, and good heat retention.

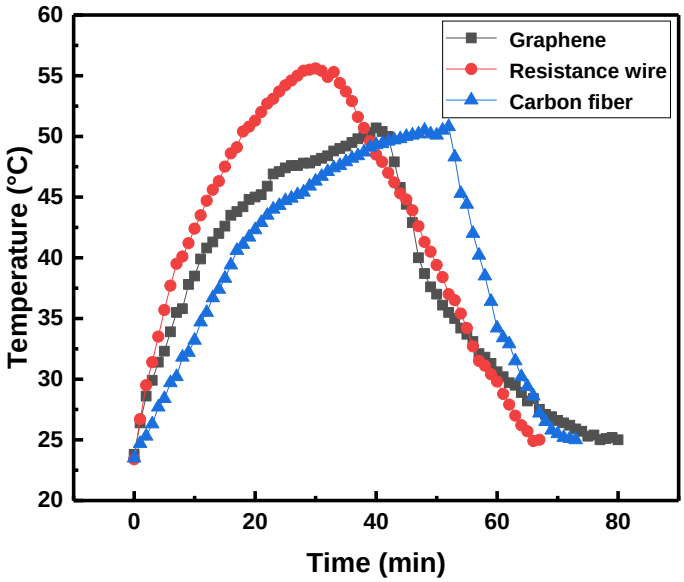

Fig. 8. Temperature-time effect diagram of three types of electrothermal composite floor

Comparison of Surface Temperature Distribution of Three Kinds of Electrothermal Composite Floors

The electrothermal composite floor with different heating materials had different heating characteristics. According to the JG/T 286 standard (2010), the inhomogeneity of temperature distribution was represented by the difference between the maximum temperature and the minimum temperature in the same surface area.

The surface temperature distributions of the electrothermal composite floor fabricated from the three heating materials were quite different. As shown in Figs. 9a, 9d, 9g, and 9j, the graphene electrothermal composite floor was uniformly heated in a planar shape, and the temperature distribution of the plate surface was relatively uniform. The three-dimensional temperature distribution cloud map showed a relatively flat temperature distribution. Most of the two-dimensional temperature distribution cloud map was orange. The average surface temperature of the floor was 49.6 °C, and the difference between the highest temperature and the lowest temperature was 4.4 °C.

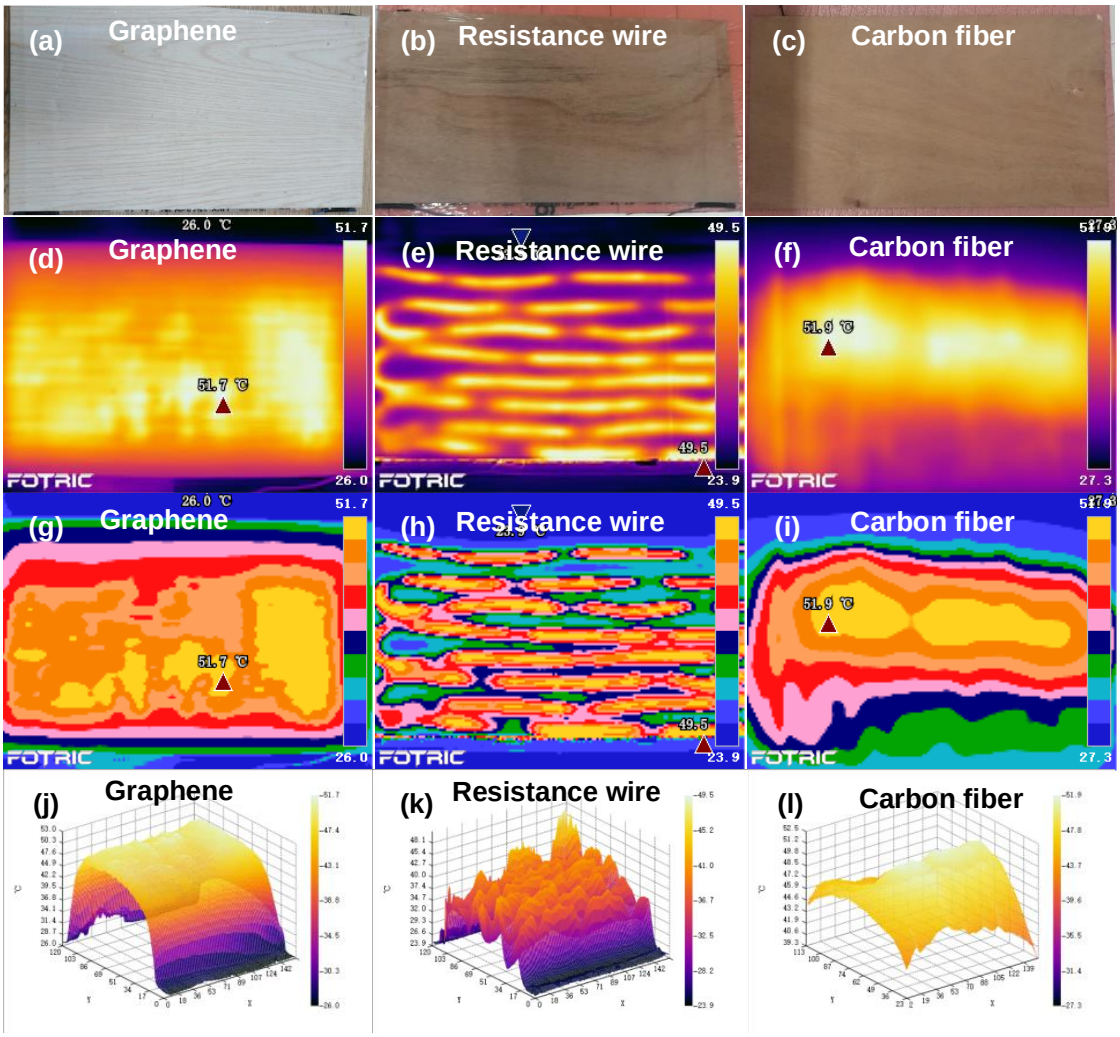

Fig. 9. a, b, c) photographs of graphene electrothermal composite floor, resistance wire electrothermal composite floor, and carbon fiber electrothermal composite floor in turn; d, e, f) infrared thermal images of three kinds of electrothermal composite floors; g, h, i) surface temperature 2D simulation of three kinds of electrothermal composite floors; j, k, l) surface temperature 3D simulation of three kinds of electrothermal composite floors.

As shown in Figs. 9b, 9e, 9h, and 9k, the temperature distribution on the surface of the carbon fiber electrothermal composite floor was not uniform. A small portion of the two-dimensional temperature distribution cloud map showed yellow. The average surface temperature of the floor was 45.3 °C, and the difference between the highest temperature and the lowest temperature was 10.1°C. As shown in Figs. 9c, 9f, 9i, and 9l, the resistance wire electrothermal composite floor was linearly heated, and the temperature distribution of the floor surface was uneven. The three-dimensional temperature distribution cloud map showed both concave and convex temperature distribution. The color difference of the two-dimensional temperature distribution cloud map was large, indicating that the temperature difference was large. The average surface temperature of the floor surface was 41.7 °C, and the difference between the highest temperature and the lowest temperature was 16.6 °C.

Table 3. Temperature Distribution Unevenness of Three Kinds of Electrothermal Composite Floor

Electrothermal Composite Floor	Temperature (°C)				Temperature Non-uniformity (°C)	Temperature Change Range (%)
	Mean	Maximum	Minimum	Difference		
Graphene	49.6	51.7	47.3	4.4	4.4	9.3
Resistance wire	41.7	49.5	32.9	16.6	16.6	50.4
Carbon fiber	45.3	51.9	41.8	10.1	10.1	24.2

The unevenness of the surface temperature distribution of the electrothermal composite floor made of the three heating materials are shown in Table 3. The resistance wire electrothermal composite floor exhibited the worst surface temperature uniformity, while the graphene electrothermal composite floor showed the best surface temperature uniformity. This was because the resistance wire had a linear heating property. The low surface temperature of the non-placed resistance wire and the high surface temperature of the placed resistance wire led to an inhomogeneous temperature profile of the resistance wire electrothermal composite floor surface. The temperature gap was too large, and the local temperature was too high during the operation, which was a certain safety hazard, while the graphene film was planarly heated. Graphene is connected to each other by equal hexagons, and the electrons are fully lapped, which reduces the interfacial thermal resistance, and the electrons move fast. Therefore, the thermal conductivity and electrical conductivities are uniform, and thermal conductivity is good. The graphene electrothermal composite floor had a uniform temperature profile with small temperature differences, which can greatly reduce the potential safety hazards of local overheating and severe heat accumulation.

The Electro-thermal Radiation Conversion Efficiency of Three Kinds of Electrothermal Composite Floors

The electro-thermal radiation conversion efficiency can be defined as the percentage of the total power input to the floor to the total radiation flux converted under the stable heating working condition of the electrothermal composite floor. Three types of electrothermal composite floors with built-in graphene heating film, carbon fiber heating film and resistance wire heating sheet were tested separately.

As shown in Table 4, the electro-thermal radiation conversion efficiency of the three types of electrothermal composite floors were quite different. According to the electro-thermal conversion in Eq. 1, the average radiation temperature was positively correlated with the electro-thermal conversion efficiency when the input power, slab area, and ambient temperature were kept constant. Among the three types of electrothermal composite floors, the average radiation temperature of graphene electrothermal composite floor was the highest, so the electro-thermal radiation conversion efficiency of graphene electrothermal composite floor was the highest. The value of η was 90.1 %, while that of resistance wire electrothermal composite floor was 58.7%, and that of carbon fiber electrothermal composite floor was 70.7%. It can be seen that the graphene electrothermal composite floor met the industry standard that the electric-thermal radiation conversion efficiency was not less than 55% in GB / T 7287 standard (2008).

Table 4. Electro-thermal Radiation Conversion Efficiency of Three Kinds of Electrothermal Composite Floor

Type of Electrothermal Composite Floor	Electrothermal Radiation Conversion Efficiency (%)
Graphene	90.1
Resistance wire	58.7
Carbon fiber	70.7

CONCLUSIONS

1. The graphene electrothermal composite floor has higher electrothermal radiation conversion efficiency, more uniform plate surface temperature distribution and smaller plate surface temperature difference, which can greatly reduce the potential safety hazards of local overheating and severe heat accumulation. The graphene electrothermal composite floor had good heating performance.
2. Under normal operating conditions at 220 V, the temperature of the surface and bottom layers of the graphene electrothermal composite floor increased with the time of energization. The temperature increase at the surface of the plate and the temperature increase at the bottom of the plate were exponentially dependent on time. After about 40 min of energization, the temperature of the surface and bottom of the graphene electrothermal composite floor tended to become stabilized. The temperature rise of the plate surface reached 25.5 °C, and the temperature of the plate bottom reached 27.3 °C, indicating that the graphene electrothermal composite floor had good heating performance.
3. The surface peak temperature of the graphene electrothermal composite floor was below 55 °C after continuous energization for 10 h, and there was no local high temperature phenomenon. The floor had a stable running performance.
4. Under normal working conditions, the temperature distribution unevenness of graphene electrothermal composite floor was 4.4 °C, which was better than 16.6 °C of resistance wire electrothermal composite floor and 10.1 °C of carbon fiber electrothermal composite floor. The surface temperature distribution of the graphene electrothermal composite floor was uniform.

5. The electro-thermal radiation conversion efficiency of graphene electrothermal composite floor was 90.1%, while that of resistance wire electrothermal composite floor was 58.7%, and that of carbon fiber electrothermal composite floor was 70.7%. The thermal radiation efficiency of the graphene electrothermal composite floor was higher.

ACKNOWLEDGMENTS

The authors thank many teachers from the school of computer and the support of the special fund for the Natural Science Foundation of Heilongjiang Province (Grant No. ZD2021E001)

REFERENCES CITED

Bao, Y. J., Huang, C. J., Chen, Y. H., and Dai, Y. (2020). "Longitudinal scale effect of electro-thermal effectiveness of front panel of the integrated wooden electric heating composite based on carbon fiber paper," *Acta Materiae Compositae Sinica* 37(12), 3214-3219 (in Chinese). DOI: 10.13801/j.cnki.fhclxb.20200402.001

Chen, W. L., Cha, W. F., Feng, X. Y., Hu, Y. M., and Feng, G. P. (2022). "Establishment of thermal order analysis method of infrared thermal imaging and study on meridian induction in graphene hyperthermia," *China Medical Device Information* 28(14), 13-16. DOI: 10.15971/j.cnki.cmdi.2022.14.053

Feng, X. Y. (2017). "Development status of graphene industry and application of heating film," *New Material Industry* 278(01), 44-47.

GB/T 41547(2022). "Solid wood composite floor," China National Standardization Administration Committee, Beijing.

GB/T 7287 (2008). "Test methods for infrared radiant heaters," China National Standardization Administration Committee, Beijing.

JG/T 286 (2010). "Low-temperature electro-thermal film," China National Standardization Administration Committee, Beijing.

Li, S. C. (2018). *Study on Structure Design and Heat Transfer Performance of Electric Composite Floor with Built-in Electrothermal Layer*, Ph.D. Dissertation, Beijing Forestry University, Beijing, China. DOI: 10.26949/d.cnki.gblyu.2018.000683

Liang, S. Q., Li, S. C., Wang, H.C., Chai, Y., and Fu, F. (2019). "Effect of thermal conductive graphite film on heat transfer performance of electrothermal parquet flooring substrate," *Journal of Northeast Forestry University* 47(08), 76-81. DOI: 10.13759/j.cnki.dlxb.2019.08.015

Liang, S. Q., Tao, X., Li, S. M., Jiang, P., Zhang, L. F., and Fu, F. (2022). "Research progress on preparation and aging resistance of carbon-based wood electrothermal composites," *Acta Materiae Compositae Sinica* 39(4), 1469-1485. DOI: 10.13801/j.cnki.fhclxb.20211123.001

Liang, S. Q., Li, S .C., Chai, Y., and Fu, F. (2018). "Process parameter optimization of electric heating engineered wood flooring," *Journal of Northeast Forestry University* 46(12), 87-93. DOI: 10.13759/j.cnki.dlxb.2018.12.016

Liu, X., Yu, Z. M., Zhang, Y., Guo, J., and Zeng, G. (2023). "Evaluation of heat transfer

performance of engineered wood flooring with built-in electric heating semi-conductive layer," *Journal of Beijing Forestry University* 45(5), 155-162. DOI: 10.12171/j.1000−1522.20220503

Song, J., Hu, H., Zhang, M., Huang, B., and Yuan, Z. (2017). "Thermal aging properties and electric heating behaviors of carbon fiber paper-based electric heating wood floors," *BioResources* 12(4), 9466-9475. DOI: 10.15376/biores.12.4.9466-9475

Ti, P., Liao, Y., Wang, Q., Qin, Z., Cai, Q., Lin, Z., and Yuan, Q. (2022). "Large-format preparation technology and electric heating performance of wooden electric heating flooring," *BioResources* 17(3), 4069-4085. DOI: 10.15376/ biores.17.3.4069-4085

Wang, J. K. (2021). *Study on the Indoor Heating Application of Graphene Electrothermal Film*, Ph.D. Dissertation, Xian University of Architecture and Technology, Xian, China. DOI: 10.27393/d.cnki.gxazu.2021.000226

Yang, C. M., Guan, B., Zhang, Z., Zhang, J., Xue, B., and Tian, X. (2023). "The establishment and numerical calculation of a heat transfer model of a graphene heating energy storage floor," *BioResources* 18(1), 1948-1970. DOI: 10.15376/biores.18.1.1948-1970

Zhou, Y. C., Li, X., Ren, C. Q., Ma, Y., Yang, C. M., Bai, Y., and Deng, Y. J. (2018). "Analysis of heat transfer effect for compound solid wood aluminum-core electro-thermal floor," *Forestry Science* 54(11), 1-6. DOI: 10.11707 /j.1001-7488.20181101

Zhou, Z. B., Zhu, Z. L., Xue, H., Li, X., Zhang, F., and Cao, P. X. (2018). "Electrothermal performance of composite floor with built-in heating layer," *Journal of Northeast Forestry University* 46(02), 53-58. DOI: 10.13759/j.cnki.dlxb.2018.02.011

Zhou, Z. B., Li, X., Ding, J. W., Guo, X. L., and Cao, P. X. (2019). "Structure design and process analysis of internal heating engineered wood flooring," *Journal of Forestry Engineering* 4(1), 165-169. DOI:10.13360 /j. issn.2096-1359.2019.01.025

Article submitted: July 6, 2023; Peer review completed: July 29, 2023; Revised version received and accepted: August 9, 2023; Published: August 11, 2023.
DOI: 10.15376/biores.18.4.6929-6943